

Blind Image Restoration Utilizing Total Variation Regularization, Shock Filter and Gradient Reliability Map

Tomio Goto, Hiroki Senshiki, Satoshi Motohashi
Dept. of Computer Science and Engineering
Nagoya Institute of Technology
Nagoya, Japan
t.goto@nitech.ac.jp

Haifeng Chen and Reo Aoki
R&D, Visual Technologies (ASIC)
EIZO Corporation
Ishikawa, Japan.

Abstract— Blind image restoration, which restores a clear latent image from a single blurred image, is an ill-posed problem to find two unknowns: 1) the latent image, and 2) the point spread function (PSF). In this paper, we propose a novel PSF estimation method utilizing total variation regularization, a shock filter and the gradient degree of reliability. The experimental results show that our proposed method delivers the best performance out of several currently available methods with respect to restoration performance. Furthermore, the processing time for our proposed method is very quick, and clear images are obtained for actual pictures.

Keywords—*Blind Image Restoration; Total Variation Regularization; Shock Filter; Gradient Degree of Reliability*

I. INTRODUCTION

Recently, digital cameras, web-cameras and smartphones have become increasingly popular ways of taking photographs. However, the quality of some pictures taken on such devices is often degraded due to image blurring caused by factors such as poor focus and camera shake. Furthermore, high-definition televisions and high-resolution displays are now widely used, with high-resolution videos being played back on such displays. And while poor focus and blurring of images is not noticeable on the small displays of mobile phones and smartphones, such lack of quality can be clearly seen when images are presented on high-resolution displays. Therefore, image restoration from degraded images is desired.

The phenomenon of image blurring stems from the characteristics of image sensors, which create images by gathering the light that falls on them when a photograph is taken. Any movement of an object or the camera during this exposure time causes image blurring. One solution is to shorten the exposure time; however, enough light needs to be obtained during the exposure, and while this presents no problem in brightly lit scenes, it does present a problem in terms of low-contrast images or blurred images being obtained in less well-lit scenes when a strobe is not used. One solution is to set the camera intensity to high, however, high image intensity values result in a high influence of shot noise, so that noisy images will be obtained.

To resolve these issues, an automatic camera-shake correction function is implemented on a lot of cameras. However, it is very expensive to design such a function and, in addition, a great deal of space is required to physically move a sensor, making it difficult to design compact cameras

incorporating such a function. As it is already difficult to reserve physical space for cameras in mobile phones and smartphones, and as space is at a premium in cameras for medical use, it is doubly difficult to implement an automatic camera-shake correction function in them. Also, such a function does nothing for degraded images that have already been taken.

Taking the above into consideration, the challenge is to find a way of restoring blurred images by using image processing. Generally, image blurring is formulated by the convolution between the latent image and the point spread function (PSF), this restoration model is based on processing restoration [1]. In this process, a blurred image is restored by utilizing a known PSF or a PSF that has been obtained by another method. This process is called “deconvolution,” with a non-blind deconvolution being one in which the PSF is known, and a blind deconvolution being one in which the PSF is unknown. In a blind deconvolution, both the latent image and the PSF are estimated by the input image, which presents an ill-posed problem. Recently, in a blind deconvolution, learning-based methods, in which an enormous database is used to solve this problem, succeeds to obtain high quality images, however, it takes long time and needs enormous database. On the other hand, a two-step solution, in which the PSF is first estimated by an input image and then the latent image is restored by the estimated PSF, achieves high-quality restoration [2], [3].

There have been many studies on two-step blind deconvolution [4]–[8]. However, for actual pictures, correct PSFs cannot be obtained in some cases, so that ringing occurs or noise is emphasized in the restored images, and there are many problems. In addition, two-step blind deconvolution requires the solving of some complex equations, which are based on the theory of probability or optimal problem with an iterative process, and this presents a problem in that it takes an enormous amount of time to solve these equations—and the restoration results depend deeply on these parameters.

In this paper, a novel algorithm based on two-step blind deconvolution is proposed. In our proposed method, during the latent image restoration step, total variation regularization [9]–[11] is applied to reduce texture components and noise; and a shock filter [12], [13] is applied to emphasize the edges, this results in an improvement of the PSF estimation performance. The method of Krishnan et al., which offers fast processing, is implemented in the deconvolution and high-speed processing is achieved. A gradient reliability map is then applied to decrease

edges, which are badly affected in the PSF estimation, to improve the performance of the PSF estimation, this is a main proposal in this paper compared with our previous work [14]. In our experiments, first the parameters for the threshold process of the gradient distributions are optimized to improve restoration performance, and then Sun's test sets [8] are used to validate our proposed method in the objective evaluations. Finally, actual blurred pictures are used to evaluate the proposed method objectively and subjectively.

II. IMAGE RESTORATION METHOD

When image blurring in an image as a whole is uniform, blurred image b is modeled as the convolution of latent image x and its PSF k as follows:

$$b = k \otimes x + n \quad (1)$$

where n is noise.

In this paper, we restore images using this blur degradation model. Image restoration can be classified as non-blind deconvolution, which is image restoration when the PSF is known; and blind deconvolution, which is image restoration when the PSF is unknown. Blind deconvolution presents the problem of having to estimate both an ideal image and its PSF from a single blurred image. In general, the final PSF is estimated by alternately repeating the latent image estimation (x-step) and its PSF estimation (k-step). The blurred image is restored by performing a final non-blind deconvolution using the estimated PSF.

III. PSF ESTIMATION ALGORITHM

Figure 1 shows an overview of our proposed method with an x-step and a k-step in PSF estimation. Alternating iterations of the PSF estimation are performed on a grayscale image of the input image. In addition, a multi-scale iterative process is used to perform the alternating iterative process while expanding gradually from a small image size to the original image size to stabilize the PSF estimation. A 3×3 Gaussian filter is used as the initial estimation of the PSF.

A. Latent Image Estimation (x-step)

In the x-step, restored image x is first obtained by deconvolution. The texture component of restored image x is removed to process the total variation regularization for noise removal. Next a shock filter is applied to the obtained structure

component to restore the edge component of the latent image x estimation.

During the deconvolution process, latent image x is restored by using the PSF k obtained by the PSF estimation process. Fast deconvolution utilizing the hyper-Laplacian priors [4] is adopted. Latent image x is determined by solving the following minimization problem.

$$x = \min_x \sum_{i=1}^N \left(\frac{\lambda}{2} (x \otimes k - b)_i^2 + \sum_{j=1}^J |(x \otimes d_j)_i|^\alpha \right) \quad (2)$$

where d is a differential filter and $|\cdot|^\alpha$ is a penalty function.

Total variation regularization is often used to decompose an image into a structure component, which consists of edges and low-frequency components; and a texture component, which consists of small oscillating signals and noise. In the ROF model [9], the evaluation function $F(u)$ is minimized to solve an image decomposition as shown in Eq. (3):

$$\inf_u F(u) = \sum_{i,j} |\nabla_{i,j}| + \lambda \sum_{i,j} |u_{i,j} - f_{i,j}|^2 \quad (3)$$

where $f_{i,j}$ is the input pixel value, $u_{i,j}$ is the computed output pixel value, i and j are pixel coordinates, and λ is a positive constant. To minimize evaluation function $F(u)$, we adopt the projection method proposed by Chambolle [10], which is known to be a fast solution. The values u and $v = f - u$ are the structure component and texture component, respectively.

The shock filter [12] is a filter for the restoration or the enhancement of signal edges by repeated calculation as shown in Eq. (4):

$$x_{t+1} = x_t - \text{sign}(\Delta x_t) \|\nabla x_t\| dt \quad (4)$$

where dt is the step-size parameter for the shock filter.

B. PSF Estimation (k-step)

In the k-step, we perform a thresholding process to obtain latent image x estimated in the x-step and estimate PSF k by solving a minimization problem by using degraded image b and ideal image x .

One specific method for a thresholding process is to divide the directions of the gradient into four groups: 0, 45, 90, and 135°. We then set the threshold α_g , which is a coefficient of a number of pixels to select for each group.

In the PSF estimation, by using observed image gradient distribution ∇b and predicted latent image gradient distribution ∇x , PSF k is estimated. By minimizing the conjugate gradient method of an energy function as shown in Eq. (5), the PSF k is estimated thusly:

$$E_k(k) = \|\nabla x' \otimes k - \nabla b\|^2 + \lambda_k \|k\|^2 \quad (5)$$

C. Gradient Degree of Reliability (R-map)

In the minimization problem for the PSF estimation of our proposed method, strong edges are used. However, those may have a negative influence due to noise or narrow signals such as impulse signals. A narrow signal, which is narrower than the blur size, causes a smaller amplitude value when the shock filter emphasizes its edge. This results in an incorrect estimation.

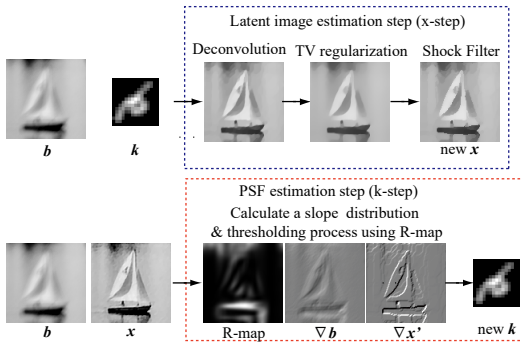


Fig. 1. Block diagram of our proposed method.

Therefore, we apply the gradient degree of reliability, which is called the R-map, as shown in Eq. (6):

$$r(x) = \frac{\|\sum_{y \in N_h(x)} \nabla b(y)\|}{\sum_{y \in N_h(x)} \|\nabla b(y)\| + 0.5} \quad (6)$$

where $N_h(x)$ is a $h \times h$ window at a center position x .

IV. EXPERIMENTAL RESULTS

To evaluate performance of our proposed PSF estimation algorithm, we experiment using Sun's test set [8]. In this evaluation, we restored 640 blurred images generated by using 80 ideal images and eight PSFs, with 1% white Gaussian noise being added to these 640 images. We then calculate the PSNR between an ideal image and its restored image. In addition, we calculate error ratio r as follows:

$$r = \frac{\|x - \tilde{x}_k\|^2}{\|x - \tilde{x}_k\|^2} \quad (7)$$

where x is an ideal image and \tilde{x}_k is the image restored by blind deconvolution. \tilde{x}_k is an image restored by non-blind deconvolution using an ideal PSF, and we refer to this non-blind deconvolution method as the "known PSF." The restoration results are better when the error ratio r approaches one. Table I shows the experimental parameters for our proposed method.

A. Objective Evaluation

Table II and Fig. 2 show the experimental results when Zoran's method [15] is used in the final non-blind deconvolution of each method, so that we evaluate only the performance of the PSF estimation. In Table II, the success rate is defined as being when $r \leq 5$, which was proposed in [16], and the restored image quality is still good. The average PSNR, the average error ratio and the success rates of our proposed method offer the best performance of currently available methods. However, the maximum error rate in Michaeli et al. method is the lowest, which implies that the method of Michaeli et al. method is a robust method. Therefore, there is some room for improvement with respect to the error ratio in our proposed method. In Fig. 2, the upper left line shows the best performance in the success rate, so our proposed method is highest compared with the other methods.

B. Subjective Evaluation for Sun's Test Set

Figures 3 and 5 show blurred images and the restored images using images of snow and a road, respectively. Figures 4 and 6 show the PSFs. Figures. (a), (b), (c) and (d) are the original blurred image, those obtained by the Michaeli et al. method, those for our previous method [14], and those for our proposed method, respectively. In Figs. 3 and 4, the snow images are not enough clear with an incorrect PSF for the Michaeli et al. method, whereas the image quality for our previous method and our proposed method is good with correct PSFs. In Figs. 5 and 6, the road images are clear enough in the Michaeli method and our proposed method, although ringing occurred in our previous method.

C. Subjective Evaluation for Actual Pictures

Figure 7 shows the blurred image and the reconstructed images using the image of a building, and Fig. 8 shows the

estimated PSFs for each method in which Krishnan et al. method is used in the final non-blind deconvolution. In Figs. 7 and 8, blurred noise remains in the image obtained using the Michaeli et al. method and our previous method, however, a clear image is obtained for our proposed method. Also, the same results are obtained for the other actual pictures.

D. Processing Time

Table III shows the processing time, which is calculated for MATLAB running on an Intel Core i5-4210M (2.60 GHz) and 8GB RAM on Windows7 for the Michaeli et al. method, our previous method and our proposed method. Table III shows the processing time for our previous method and our proposed method is almost the same, and both are more than 116 times faster than that for the Michaeli et al. method.

TABLE I. EXPERIMENTAL PARAMETERS FOR OUR PROPOSED METHOD.

| | | | |
|---------------------------------|-------------------|------------------|---------|
| PSF size | | | 31 x 31 |
| Iterative number at each scale | | | 5 |
| Latent image estimation process | Deconvolution | λ_d | 1500 |
| | TV Regularization | Iterative number | 10 |
| | | λ_d | 20 |
| | Shock Filter | Iterative number | 1 |
| | | Dt | 1.0 |
| PSF estimation process | Iterative number | | 30 |
| | Threshold value | | 0.05 |
| | α_g | | 40 |

TABLE II. EXPERIMENTAL RESULTS OF OBJECTIVE EVALUATIONS.

| Methods | Average PSNR [dB] | Average Error Ratio | Max Error Ratio | Success Rates [%] ($r \leq 5$) |
|--------------------------|-------------------|---------------------|-----------------|----------------------------------|
| Blur input | 24.62 | 6.86 | 25.92 | 35.63 |
| Known PSF | 32.33 | 1.00 | 1.00 | 100.00 |
| Cho & Lee [5] | 26.65 | 9.00 | 118.28 | 68.26 |
| Xu & Jia [6] | 29.19 | 3.08 | 65.36 | 88.63 |
| Sun et al. [7] | 30.20 | 2.14 | 24.98 | 93.71 |
| Michaeli & Irani [16] | 29.06 | 2.38 | 9.23 | 95.47 |
| Our previous method [14] | 30.21 | 2.23 | 48.39 | 93.44 |
| Proposed method | 30.88 | 1.64 | 27.18 | 97.19 |

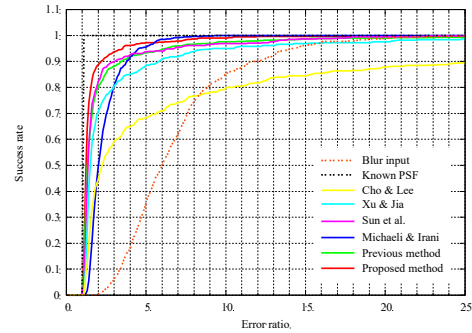


Fig. 2. Experimental results of cumulative error rate.

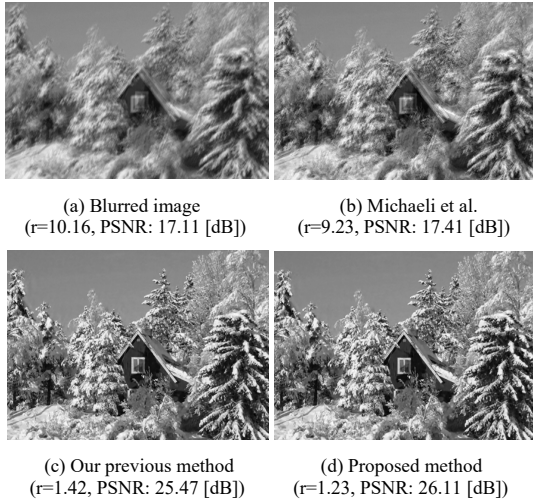


Fig. 3. Blurred image and restored images (Snow image).

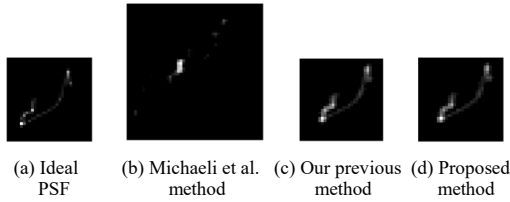


Fig. 4. Ideal PSF and estimated PSFs (Snow image).

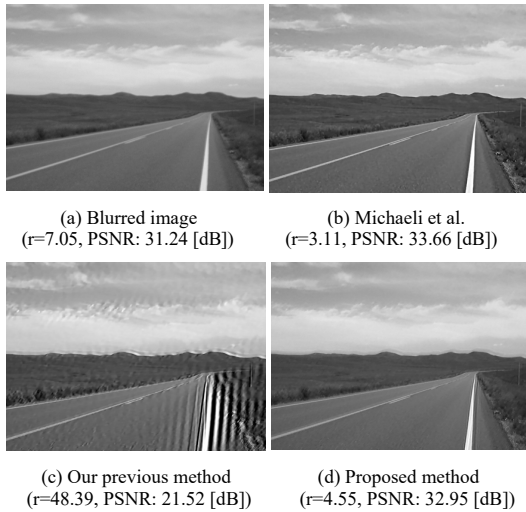


Fig. 5. Original image and restored images (Road image).

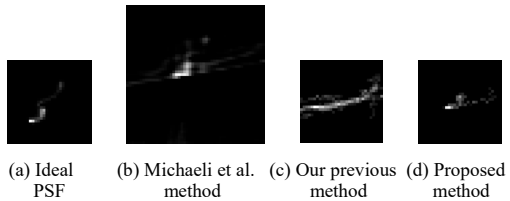


Fig. 6. Ideal PSF and estimated PSFs (Road image).

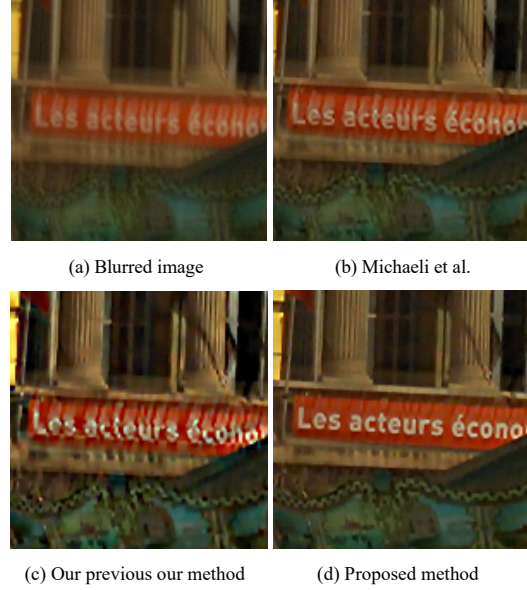


Fig. 7. Original image and restored images (Building image).

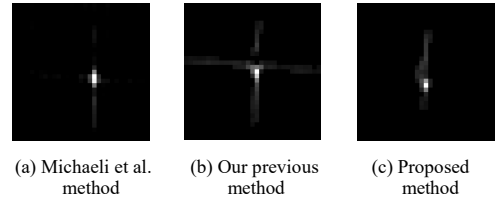


Fig. 8. Estimated PSFs (Building image).

TABLE III. PROCESSING TIME [SEC].

| Experimental image | Image size | Michaeli et al. | Our previous method | Proposed method |
|--------------------|------------|-----------------|---------------------|-----------------|
| Building | 716 × 451 | 2596.0 | 22.3 | 22.6 |
| Lyndsey | 724 × 905 | 4498.1 | 39.0 | 39.6 |

V. CONCLUSION

In this paper, we proposed a novel PSF estimation method utilizing total variation regularization, a shock filter and the gradient degree of reliability. The results of the experiment clearly show that we achieved the best performance for average PSNR, average error ratio, and success rate in the objective evaluation. The clearest images were obtained in the Sun's test set and for an actual image in the subjective evaluation. Also, the processing time of our proposed method was 116 times faster than that of the Michaeli et al. method. Thus, our proposed method clearly offers state-of-the-art performance. For further research, we intend to improve the maximum error ratio, which was decreased because there were a few restored failure images using our proposed method, and it will be achieved to select optimized parameters of total variation regularization.

REFERENCES

- [1] R. Fergus, B. Singh, A. Hertzmann, S. T. Roweis and W. T. Freeman: "Removing Camera Shake from a Single Image", *ACM Trans. on Graphics (SIGGRAPH)*, Vol. 25, No. 3, pp.784–794, 2006.
- [2] Q. Shan, J. Jia and A. Agarwala: "High-quality Motion Deblurring from a Single Image", *ACM Transaction on Graphics (SIGGRAPH)*, Vol. 27, No. 3, pp.73:1–10, Aug. 2008.
- [3] A. Levin, Y. Weiss, F. Durand and W. T. Freeman: "Understanding and Evaluating Blind Deconvolution Algorithms", *IEEE International Conference on Computer Vision and Pattern Recognition (CVPR)*, pp.1964–1971, Jun. 2009.
- [4] D. Krishnan and R. Fergus: "Fast Image Deconvolution using Hyper-Laplacian Prior", *Proc. of Neural Information Processing Systems (ANIPS)*, pp.1033–1041, Dec. 2009.
- [5] S. Cho and S. Lee: "Fast Motion Deblurring", *ACM Transaction on Graphics*, Vol. 28, No. 5, Article No. 145, Dec. 2009.
- [6] L. Xu and J. Jia: "Two-Phase Kernel Estimation for Robust Motion Deblurring", *European Conference on Computer Vision (ECCV)*, pp.57–170, Sep. 2010.
- [7] A. Levin, Y. Weiss, F. Durand and W. T. Freeman: "Efficient Marginal Likelihood Optimization in Blinddeconvolution", *IEEE International Conference on Computer Vision and Pattern Recognition (CVPR)*, pp.2657–2664, Jun. 2011.
- [8] L. Sun, S. Cho, J. Wang and J. Hays: "Edge-based Blur Kernel Estimation Using Patch Priors", *IEEE International Conference on Computational Photography (ICCP)*, pp.1–8, Apr. 2013.
- [9] S. J. Osher and E. Fatemi: "Nonlinear Total Variation Based Noise Removal Algorithms", *Physica D*, Vol. 60, pp.259–268, 1992.
- [10] A. Chambolle: "An Algorithm for Total Variation Minimization and Applications", *J. Mathematical Imaging and Vision*, Vol. 20, No. 1, pp.89–97, 2004.
- [11] A. Beck and M. Teboulle: "Fast Gradient-Based Algorithms for Constrained Total Variation Image Denoising and Deblurring Problems", *IEEE Transactions on Image Processing*, Vol. 18, No. 11, pp.2419–2434, Nov. 2009.
- [12] S. J. Osher and L. I. Rudin: "Feature-Oriented Image Enhancement using Shock Filters", *SIAM Journal on Numerical Analysis*, Vol. 27, pp.910–940, 1990.
- [13] J. G. M. Schavemaker, M. J. T. Reinders, J. J. Gerbrands, and E. Backer: "Image Sharpening by Morphological Filtering", *Elsevier Pattern Recognition*, Vol. 33, No. 6, pp.997–1012, Jun. 2000.
- [14] H. Senshiki, S. Motohashi, T. Goto, H. Chen and R. Aoki: "PSF Estimation Using Total Variation Regularization and Shock Filter for Blind Deconvolution", *IEEE International Conference on Consumer Electronics (ICCE)*, pp.479–480, Jan. 2017.
- [15] D. Zoran and Y. Weiss: "From Learning Models of Natural Image Patches to Whole Image Restoration", *IEEE International Conference on Computer Vision (ICCV)*, pp.479–486, Nov. 2011.
- [16] T. Michaeli and M. Irani: "Blind Deblurring Using Internal Patch Recurrence", *European Conference on Computer Vision (ECCV)*, pp.783–798, Sep. 2014.